

An Advanced Neutron Absorbing Ti-Gd Alloy: Part 2-Oxide Properties in Boric Acid

Do Haeng Hur*, Young-Bum Chun

Nuclear Materials Research Division, Korea Atomic Energy Research Institute, Daejeon 34057

*Corresponding author: dhhur@kaeri.re.kr

***Keywords** : neutron absorbing material, Ti-Gd alloy, electrochemical impedance spectroscopy, Mott-Scottky relation

1. Introduction

A spent nuclear fuel (SNF) assembly is located in a storage unit cell that forms racks in a spent fuel pool and baskets in a dry storage cask. Because SNF continues to decay and emit considerable heat during storage, neutron absorber materials are required to maintain SNF safely under a subcritical condition. Therefore, these materials must have high thermal neutron absorbing capability and thermal conductivity. High mechanical strength is also needed for high-density storage under adequate criticality control. It would be even more ideal if the materials have a reduced weight and an improved workability.

Recently, we have launched a research program on the development of new dual-purpose materials with both neutron absorbing and structural function. Ti-Gd alloys with different Gd contents were fabricated and the corrosion behavior of the alloys was investigated in boric acid at 50 °C using electrochemical and immersion corrosion tests, which was reported in Part 1 [1]. The corrosion behavior of an alloy is affected by the oxide properties formed on the alloy surface [2]. Therefore, we report here the oxide properties of Ti-Gd alloys formed during the immersion corrosion tests.

2. Materials and Methods

2.1 Material Preparation

Pure Ti and Ti-Gd alloys with different Gd content were fabricated with Ti and Gd lumps by plasma arc melting in a chamber filled with argon gas at a pressure of 200 kPa. The ingots were soaked at 1150 °C for 30 min and then hot-forged. The forged bars were hot-rolled at 1000 °C with a thickness reduction of ~50%. The plates were finally heat-treated at 1000 °C for 40 min and air-cooled. The chemical compositions of the materials are listed in Table 1.

Table 1: Chemical compositions of test materials

Material	Ti	Gd (wt. %)	O (wt. ppm)	N (wt. ppm)
Pure Ti	Balance	0	1040	2
Ti-3Gd	Balance	2.97	900	6
Ti-5Gd	Balance	4.81	980	4
Ti-10Gd	Balance	9.68	1000	N.D.

2.2 Immersion Corrosion Tests

Immersion corrosion tests were performed in boric acid solution with 3,000 wt. ppm B at 50 °C. The solution was not deaerated to simulate a pool storage condition. The corrosion coupons were removed from the corrosion cell every 500 h, rinsed in deionized water, and dried with compressed air. After weight measurement, the coupons were returned to the cell filled with new test solution. The total test duration was 1500 h.

2.3 Characterization of Oxides

After the immersion corrosion tests for 1500 h, cross-sections of the oxide layers formed on specimens were extracted using the focused ion beam (FIB) milling technique with a gallium ion beam at a beam energy of 30 keV. The cross-sectional images of the oxide layers were observed using a transmission electron microscope (TEM) and the chemical compositions of the layers were examined using EDS built in the TEM at an accelerating voltage of 200 kV.

2.4 Electrochemical Tests

Electrochemical impedance spectroscopy (EIS) was used to measure the electrochemical properties of oxide films formed on specimens during the immersion tests for 1500 h. The EIS test was performed in a borated buffer solution (0.05 M H₃BO₃ + 0.075 M Na₂B₄O₇) at 50 °C. Oxygen dissolved in the solution was removed by continuous blowing of ultra-high purity nitrogen gas at a rate of 100 mL/min during the test. After the open circuit potential (OCP) of each specimen was stabilized, EIS measurements were conducted in a frequency range from 100 kHz to 10 mHz at the OCP using an amplitude of 10 mV rms.

Capacitances of oxide films formed during the immersion corrosion tests for 1500 h were measured in a borated buffer solution (0.05 M H₃BO₃ + 0.075 M Na₂B₄O₇) at 50 °C. The solution was deaerated as described above. After the electrode potential reached a stable OCP, capacitance measurement was started at a fixed frequency of 1000 Hz with an amplitude of 10 mV rms. The potential was applied in the negative direction from +2.0 V to -1.5 V vs. the OCP with a potential step of 20 mV.

3. Results and Discussion

3.1 Structure and Chemical Compositions of Oxides

As shown in Fig. 1, the cross-sectional TEM images of the oxides revealed that extremely thin, compact and uniform TiO₂ films were formed on the top of the alloy matrix. The thicknesses of the films were approximately 6–7 nm, irrespective of the samples. Crystalline lattice fringes were clearly visible in the matrix, while a distinct lattice images were not observed in the oxide films, suggesting that the films are amorphous. The O signal decreased gradually as the Ti signal increased when the electron beam was scanned towards the matrix. Gd was additionally detected in the film of Ti-10Gd, but its content was minor up to 0.52 at. %.

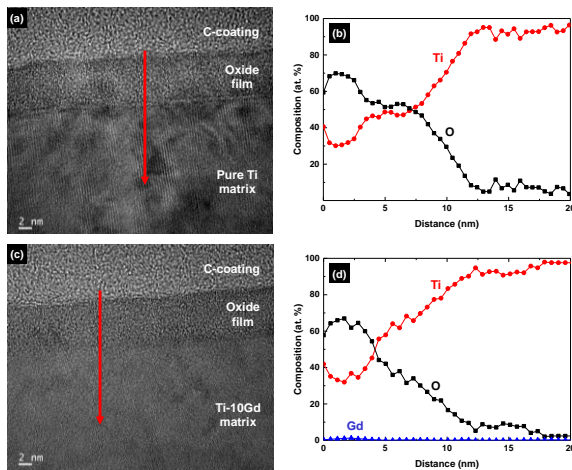


Fig. 1. Cross-sectional TEM images and EDS line profiles of (a, b) pure Ti and (c, d) Ti-10Gd.

3.2 EIS Responses of Oxide Films

Fig. 2 shows the Nyquist and Bode plots of the specimens exposed to the boric acid solution at 50 °C for 1500 h. As shown in the Nyquist diagram, there is no obvious difference of the semicircles in all the range of frequencies tested. However, the impedance value was the largest for pure Ti and decreased in the following order: pure Ti > Ti-3Gd > Ti-10Gd, especially in the low frequency region. This indicates that the charge transfer of the Faradaic current is facilitated in Ti-Gd alloys, resulting in a higher corrosion rate of the alloys. As seen in the Bode diagram, the impedance values showed a linear relationship with frequency in the frequency regions below approximately 100 Hz, and then approached a constant value in the higher frequency region. The phase angle was a constant of about -81° in the low frequency region below 3 Hz, and then increased gradually to approach zero at higher frequencies. It is evident that the EIS responses observed in low and high frequency regions reflect the typical behavior of a capacitor and a resistor, respectively. Therefore, the EIS data was

further interpreted using an equivalent circuit shown in Fig. 2c.

A significant reduction of the charge transfer resistance (R_{ct}) was observed in Ti-Gd alloys, indicating that the transfer of Faradaic current across the double layer was facilitated, in good agreement with the results of the electrochemical and immersion corrosion tests (See Part 1). Electrical resistance of oxide films (R_f) was also reduced in the films of Ti-Gd alloys, resulting in higher corrosion rates.

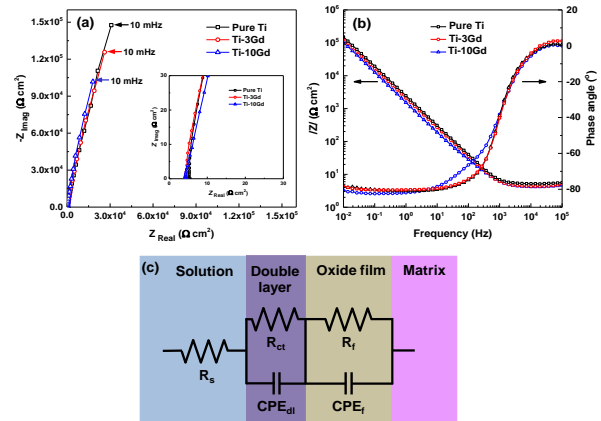


Fig. 2. EIS spectra of oxide films formed on pure Ti and Ti-Gd alloys in the boric acid solution at 50 °C for 1500 h: (a) Nyquist plot, (b) Bode plot, and (c) equivalent circuit model.

3.3 Mott-Schottky (M-S) Behavior of Oxide Films

Fig. 3 shows the M-S plots of oxide films formed during the immersion tests for 1500 h. The capacitance values increased with the increase of Gd content. The M-S plots exhibited linear positive slopes that are characteristic of an n-type semiconductor. The donor concentrations calculated using the M-S relation [3] are listed in Table 1. The total donor concentrations of the oxide films in region I and II increased by ~30% for Ti-3Gd, ~40% for Ti-5Gd, and ~75% for Ti-10Gd, compared to that of pure Ti. This indicates that the oxide films formed on Ti-Gd alloys with a higher Gd content contain a greater point defect density that carries the charges through the films

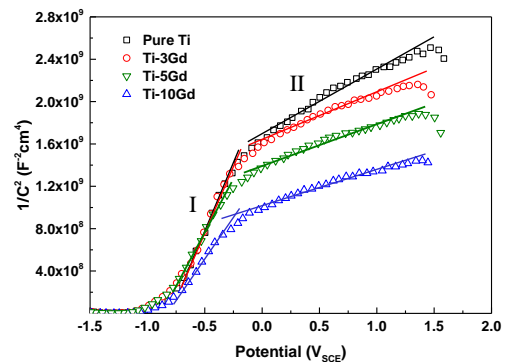


Fig. 3. Mott-Schottky plots of oxide films formed on pure Ti and Ti-Gd alloys in the boric acid solution at 50 °C for 1500 h.

Table 1: Donor concentrations in the oxide films calculated by the Mott-Schottky relation

	Region I (10^{21} cm^{-3})	Region II (10^{21} cm^{-3})	Total (10^{21} cm^{-3})
Pure Ti	1.05	4.85	5.90
Ti-3Gd	1.10	6.62	7.72
Ti-5Gd	1.37	6.74	8.11
Ti-10Gd	1.71	8.57	10.3

Metal cations and oxygen anions are known to migrate through point defects in oxide films [4,5]. The higher the donor concentration, the higher the current flow. Consequently, the corrosion rate and the passive current density of Ti-Gd alloys will be higher than those of pure Ti. The M-S behavior is consistent with the EIS responses shown in Fig. 2. In other words, the increased defect density will deteriorate the oxide film resistance and thus facilitate charge transfer across both the film and double layer, thereby leading to an increase of the corrosion rate.

4. Conclusions

Amorphous and n-type semiconducting TiO_2 films were formed on pure Ti and Ti-Gd alloys in boric acid solution at 50 °C. The oxide films of Ti-Gd alloys exhibited a lower electrical film resistance, lower charge transfer resistance, and higher donor density compared to those of pure Ti. Therefore, a higher corrosion and passive current density, and greater weight loss of the alloys (See Part 1) are, in part, attributed to the characteristics of the oxide films.

5. Acknowledgements

This study was financially supported by the Korea Atomic Energy Research Institute R&D program with a contract number of 524480-23.

REFERENCES

- [1] D.H. Hur, Y.B. Chun, An advanced neutron absorbing Ti-Gd alloy: Part 1-corrosion behavior in boric acid, Transactions of the Korean Nuclear Society Autumn Meeting, Gyeongju, Korea, October 26-27, 2023.
- [2] D.-S. Lim, S.-H. Jeon, B.J. Bae, J. Choi, K.M. Song, D.H. Hur, Effect of zinc addition scenarios on general corrosion of Alloy 690 in borated and lithiated water at 330 °C, Corros. Sci. 189 (2021), 109627.
- [3] L.V. Taveira, M.F. Montemor, M. Da Cunha Belo, M.G. Ferreira, L.F.P. Dick, Influence of incorporated Mo and Nb on the Mott-Schottky behavior of anodic films formed on AISI 304L, Corros. Sci. 52 (2010) 2813–2818.
- [4] C.Y. Chao, L.F. Lin, D.D. Macdonald, A point defect model for anodic passive films, J. Electrochem. Soc. 128 (1981) 1187–1194.

- [5] D.D. Macdonald, The history of the point defect model for the passive state: a brief review of film growth aspects, Electrochim. Acta 56 (2011) 1761–1772.